A Relaxed Problem of Registration Based on the Saint Venant-Kirchhoff Material Stored Energy for the Mapping of Mouse Brain Gene Expression Data to a Neuroanatomical Mouse Atlas

Ratiba Derfoul[1,2] and Carole Le Guyader[1]
{ratiba.derfoul,carole.le-guyader}@insa-rouen.fr

[1] Laboratoire de Mathématiques, INSA de Rouen, Saint-Étienne-du-Rouvray, France
[2] IFP Énergies nouvelles, Rueil-Malmaison, France

Abstract. In this paper, we address the issue of designing a theoretically well-motivated registration model capable of handling large deformations. Motivated by the fine properties of the Saint Venant-Kirchhoff material, we propose a variational model combining a measure of dissimilarity and a regularizer based on the stored energy of such a material. We prove the existence of generalized solutions of this problem. We then describe and analyze a numerical method of resolution based on the introduction of an associated decoupled problem under inequality constraint in which an auxiliary variable simulates the Jacobian matrix of the deformation field. A theoretical result is established and we investigate the efficiency of the proposed matching model for the registration of mouse brain gene expression data to a neuroanatomical mouse atlas.

Keywords: Image registration, calculus of variations, nonlinear elasticity, Saint Venant-Kirchhoff materials, relaxed problem, decoupled problem, theoretical convergence, mouse atlas

1 Introduction

Given two images called Template and Reference, registration consists in determining an optimal diffeomorphic transformation φ such that the deformed Template image is aligned with the Reference. This technique has gained much interest in clinical studies among others, when comparing an image to a database or for volumetric purposes. For images of the same modality, the goal of registration is to correlate the geometrical features and the intensity level distribution of the Reference and those of the Template. When the images have been acquired through different mecanisms and have different modalities, registration aims to correlate both images while preserving the modality of the Template image.
There are forward and backward registrations. In this work, we adopt the Eulerian framework to find a backward transformation Φ such that the grid points y

in the deformed Template originate from non-grid points $x = \Phi(y)$.
For an overview of existing parametric and non-parametric registration methods (including landmarks, L^2 similarity, linear elasticity, linear diffusion, splines, viscous fluid model, etc.), we refer the reader to [17]. In the case of non-parametric methods (our framework), the transformation is not restricted to a parameterizable set and the problem is phrased in terms of minimization of functional (with unknown the deformation vector field φ) including a distance measure criterion and a smoother on the deformation vector field φ. Physical arguments often motivate the way the smoother is devised. Classical regularizers such as linear elasticity (see [4]) are not suitable for problems involving large deformations since assuming small strains and the validity of Hooke's law. The scope of the proposed work is thus to devise a theoretically well-motivated registration model in a variational formulation, authorizing large and smooth deformations, while keeping the deformation map topology-preserving.
For problems involving large deformations but by a different approach from ours, we refer the reader to [5] in which Christensen et al. propose a viscous fluid model (not in a variational form). The objects to be matched are viewed as fluids evolving in accordance with the fluid dynamic Navier-Stokes equations. More precisely, given the force field f, the deforming image is considered to be embedded in a viscous fluid whose motion is governed by Navier-Stokes equations for conservation of momentum:

$$\mu \triangle v(x,t) + (\nu + \mu)\nabla\ (\nabla \cdot v(x,t)) = f(x, u(x,t)), \tag{1}$$

$$v(x,t) = \partial_t u(x,t) + \nabla u(x,t) \cdot v(x,t). \tag{2}$$

Equation (2), defining material derivative of the displacement field u, nonlinearly relates the velocity v and the displacement vector field. Constants μ and ν are viscosity coefficients of the fluid. One drawback of this method is the computational cost. Numerically, the image-derived force field $f(x, u(x,t))$ is first computed at time t. Fixing the force field f, linear equation (1) is solved for $v(x,t)$ numerically using the successive over-relaxation scheme. Then an explicit Euler scheme is used to advance u in time. These elements motivated us to propose an alternative framework requiring faster implementation.
We now depict the mathematical setting. Let us emphasize that the focus of the paper is on the mathematical presentation and well-posedness of a nonlinear elasticity-based registration model. Hence, the computational results are currently restricted to mouse brain gene expression data. Later work may go to a larger range of medical images with comparisons to reference methods.
Let Ω be a connected bounded open subset of $\mathbb{R}^2$ with Lipschitz boundary $\partial\Omega$ representing the reference configuration. Let us denote by $R : \bar{\Omega} \to \mathbb{R}$ the Reference image and by $T : \bar{\Omega} \to \mathbb{R}$ the Template image. It is assumed that T and R are both defined on the open and bounded domain Ω in the plane, a rectangle in general. Also, for theoretical and numerical purposes, we assume that T is compactly supported on Ω to ensure that $T \circ \varphi$ is always defined and we assume that T is Lipschitz continuous with Lipschitz constant $K > 0$. Also, R is supposed to be sufficiently smooth.

Let $\varphi : \bar{\Omega} \to \mathbb{R}^2$ be the deformation of the reference configuration. A deformation is a smooth enough mapping that is orientation-preserving and injective, except possibly on $\partial\Omega$. We also denote by u the associated displacement such that $\varphi = Id + u$. The deformation gradient is $\nabla\varphi = I_2 + \nabla u$, $\bar{\Omega} \to M_2(\mathbb{R})$, the set $M_2(\mathbb{R})$ being the set of all real square matrices of order 2. Thus the idea is to find a smooth deformation field φ such that the deformed Template matches the Reference. The model is phrased as a functional minimization problem whose unknown is φ. It combines a distance measure criterion chosen to be the L^2-norm of the difference between the deformed Template and the Reference, and a smoother on the deformation field. An alternative to intensity-based measures would consist in using information-theoretic-based matching measures such as mutual information (see [17]), suitable when dealing with images of different modalities or in comparing, for instance, the normalized gradient fields of both images (see [8] and [11]).
The proposed matching criterion is complemented by a regularizer on the deformation field φ. To allow large deformations, we introduce a nonlinear-elasticity-based smoother, the theory of linear elasticity being unsuitable in this case since assuming small strains and the validity of Hooke's law. We propose to view the shapes to be warped as isotropic, homogeneous, hyperelastic materials and more precisely as Saint Venant-Kirchhoff materials. Note that rubber, filled elastomers, biological tissues are often modeled within the hyperelastic framework, which motivates our modelling.
For the sake of completeness, we would like to refer the reader to previous works related to registration based on nonlinear elasticity principles. In [8], Droske and Rumpf address the issue of non-rigid registration of multi-modal image data. The matching criterion includes first order derivatives of the deformation and is complemented by a nonlinear elastic regularization based on a polyconvex stored energy function, which is different from our proposed approach. We also mention the combined segmentation/registration model introduced by Le Guyader and Vese ([12]) in which the shapes to be matched are viewed as Ciarlet-Geymonat materials, the works [2] and [16] for a variational registration method for large deformations (Large Deformation Diffeomorphic Metric Mapping - LDDMM), and refer to [20] for a much related work that also uses nonlinear elasticity regularization but implemented by the finite element method.

Before depicting the mathematical material, we review some fundamental concepts and notations (see [6] for further details). We recall that the right Cauchy-Green strain tensor is defined by $C = \nabla\varphi^T\nabla\varphi = F^TF \in \mathcal{S}^2$ with $\mathcal{S}^2 = \left\{A \in M_2(\mathbb{R}), A = A^T\right\}$, set of all real symmetric matrices of order 2. Physically, the right Cauchy-Green tensor can be interpreted as a quantifier of the square of local change in distances due to deformation. The Green- Saint Venant strain tensor is defined by $E = \frac{1}{2}\left(\nabla u + \nabla u^T + \nabla u^T\nabla u\right)$. Associated with a given deformation φ, it is a measure of the deviation between φ and a rigid deformation. We also need the following notations: $A : B = \mathrm{tr}A^TB$ the matrix inner product in $\mathbb{R}^2$ and $||A|| = \sqrt{A : A}$, matrix norm in $\mathbb{R}^2$ (Frobenius

norm). The stored energy of an isotropic, homogeneous, hyperelastic material, if the reference configuration is a natural state, is of the form:

$$W(F) = \widehat{W}(E) = \frac{\lambda}{2} \left(\operatorname{tr} E\right)^2 + \mu \operatorname{tr} E^2 + o\left(||E||^2\right), \; F^T F = I + 2E. \quad (3)$$

The stored energy function of a Saint Venant-Kirchhoff material is defined by $W_{SVK}(F) = \widehat{W}(E) = \frac{\lambda}{2} \left(\operatorname{tr} E\right)^2 + \mu \operatorname{tr} E^2$. The Saint Venant-Kirchhoff material is thus the simplest one that agrees with expansion (3). Moreover, as suggested in [12] or [14], from a numerical viewpoint, this modelling can generate high-magnitude deformations. These two arguments motivate the choice of the model we propose. At last, to ensure that the distribution of the deformation Jacobian determinants does not exhibit too large contractions or too large expansions, we propose to complement the model by a term controlling that the Jacobian determinant remains close to 1. In definitive, we propose to consider the following minimization problem:

$$\inf \left\{ I(\varphi) = \int_\Omega f(x, \varphi(x), \nabla\varphi(x))\, dx \; : \; \varphi \in \mathrm{Id} + W_0^{1,4}(\Omega, \mathbb{R}^2) \right\}, \text{ with} \quad (4)$$

$f(x, \varphi, \xi) = \frac{\nu}{2} \left(T(\varphi) - R\right)^2 + W_{SVK}(\xi) + \mu \left(\det\xi - 1\right)^2 = \frac{\nu}{2} \left(T(\varphi) - R\right)^2 + W(\xi)$. Also, $\varphi \in \mathrm{Id} + W_0^{1,4}(\Omega, \mathbb{R}^2)$ means that $\varphi = \mathrm{Id}$ on $\partial\Omega$ and $\varphi \in W^{1,4}(\Omega, \mathbb{R}^2)$. $W^{1,4}(\Omega, \mathbb{R}^2)$ denotes the Sobolev space of functions $\varphi \in L^4(\Omega, \mathbb{R}^2)$ with distributional derivatives up to order 1 which also belong to $L^4(\Omega)$. (We justify later that $W^{1,4}(\Omega, \mathbb{R}^2)$ is a suitable functional space for the considered problem).

2 Theoretical Results

2.1 Introduction of the Relaxed Problem

Function f in (4) fails to be quasiconvex, which raises a drawback of theoretical nature since we cannot obtain the weak lower semi-continuity of the functional. The idea is thus to replace problem (4) by the so-called associated relaxed problem (QP) formulated in terms of the quasiconvex envelope of f. Even though the original f is not quasiconvex and therefore in general the infimum of (4) is not attained, one has $\inf(4) = \inf(QP)$ and with some extra coercivity condition, the infimum of (QP) is reached. To the best of our knowledge, this technique of relaxation has never been used in the context of image registration before.
In the sequel, we start by establishing the explicit expression of the quasiconvex envelope of f and derive the associated relaxed problem.

Proposition 1. *The relaxed problem associated to (4) is defined by:*

$$\inf \left\{ \bar{I}(\varphi) = \int_\Omega Qf(x, \varphi(x), \nabla\varphi(x))\, dx \; : \; \varphi \in Id + W_0^{1,4}(\Omega, \mathbb{R}^2) \right\}, \quad (5)$$

with Qf *given by:* $Qf(x,\varphi,\xi) = \begin{cases} \dfrac{\nu}{2}\,(T(\varphi)-R)^2 + W(\xi) \;\; \textit{if } ||\xi||^2 \geq 2\dfrac{\lambda+\mu}{\lambda+2\mu}, \\ \dfrac{\nu}{2}\,(T(\varphi)-R)^2 + \Psi(det\xi) \;\; \textit{if } ||\xi||^2 < 2\dfrac{\lambda+\mu}{\lambda+2\mu}, \end{cases}$

and Ψ *the convex mapping such that* $\Psi : t \mapsto -\dfrac{\mu}{2}\,t^2 + \mu\,(t-1)^2 + \dfrac{\mu(\lambda+\mu)}{2(\lambda+2\mu)}$.

Proof. By definition (see Chapter 9, p. 432 of [7]), for almost every $x \in \Omega$ and for every $(\varphi,\xi) \in \mathbb{R}^2 \times \mathbb{R}^4$, the quasiconvex envelope of f with respect to the last variable is defined by:

$$Qf(x,\varphi,\xi) = \inf\left\{ \frac{1}{\text{meas}(D)} \int_D f(x,\varphi,\xi+\nabla\Phi(y))\,dy \;:\; \Phi \in W_0^{1,\infty}(D,\mathbb{R}^2) \right\},$$

$D \subset \mathbb{R}^2$ being a bounded open set. Consequently, in our case, $Qf(x,\varphi,\xi) = \dfrac{\nu}{2}\,(T(\varphi)-R)^2 + QW(\xi)$.
After some intermediate computations, one has $W(\xi) = \beta\,\left(||\xi||^2-\alpha\right)^2 + \Psi(\det\xi)$ with $\alpha = 2\dfrac{\lambda+\mu}{\lambda+2\mu}$ and $\beta = \dfrac{\lambda+2\mu}{8}$. From Theorem 3.1, p. 35 of [3], the result is straightforward. This judicious rewriting of $W(\xi)$ allows to see that $W^{1,4}(\Omega,\mathbb{R}^2)$ is a suitable functional space for φ: from generalized Hölder's inequality, if $\varphi \in W^{1,4}(\Omega,\mathbb{R}^2)$, then $\det\nabla\varphi \in L^2(\Omega)$.

It now remains to be proved that the infimum of (QP) is attained and that if $\bar{\varphi}$ is a solution of (5), then there exists a minimizing sequence $\{\varphi_\nu\}$ of (4) such that φ_ν weakly converges to $\bar{\varphi}$ and $I(\varphi_\nu) \to \bar{I}(\bar{\varphi})$. The solutions of (5) are considered as generalized solutions of (4), in the sense of weak convergence.

2.2 Existence of Minimizers for the Relaxed Problem and Relaxation Theorem

We now state the main theoretical result.

Theorem 1. *The infimum of (5) is attained. Let then* $\bar{\varphi} \in W^{1,4}(\Omega,\mathbb{R}^2)$ *be a minimizer of the relaxed problem (5). Then there exists a sequence* $\{\varphi_\nu\}_{\nu=1}^{\infty} \subset \bar{\varphi} + W_0^{1,4}(\Omega,\mathbb{R}^2)$ *such that* $\varphi_\nu \to \bar{\varphi}$ *in* $L^4(\Omega,\mathbb{R}^2)$ *as* $\nu \to \infty$ *and* $I(\varphi_\nu) \to \bar{I}(\bar{\varphi})$ *as* $\nu \to \infty$. *Moreover, the following holds:* $\varphi_\nu \rightharpoonup \bar{\varphi}$ *in* $W^{1,4}(\Omega,\mathbb{R}^2)$ *as* $\nu \to \infty$.

Proof. The proof of existence of minimizers of (5) is based on Theorem 8.29, p. 404, Chapter 8 of [7] (theorem due to Acerbi-Fusco [1] and Marcellini [15]) and rests upon the derivation of the following coerciveness and continuity double inequality:

$$C_3\,||\xi||^4 - C_4 \leq Qf(x,\varphi,\xi) \leq \left(\beta + \frac{\mu}{2}\right)||\xi||^4 + 4K^2||\varphi||^2 + C_2,$$

with C_3 a positive constant and with C_2 and C_4 two non-negative constants.
The proof of the second part of the theorem is based on Theorem 9.8, p. 432, Chapter 9 of [7].

We now propose a numerical method for the resolution of the relaxed problem. It is motivated by a related prior work by Negrón Marrero ([18]).

3 A Numerical Method of Resolution

3.1 Description and Analysis of the Proposed Numerical Method

In [18], Negrón Marrero describes and analyzes a numerical method that detects singular minimizers and avoids the Lavrentiev phenomenon for three dimensional problems in nonlinear elasticity. This method consists in decoupling the function φ from its gradient and in formulating a related decoupled problem under inequality constraint. In the same spirit, we introduce an auxiliary variable V simulating the Jacobian deformation field $\nabla\varphi$ (-the underlying idea being to remove the nonlinearity in the derivatives of the deformation-) and derive a functional minimization problem phrased in terms of the two variables φ and V. Nevertheless, our approach is different from the one in [18] in several points: in [18], the author focuses on the decoupled discretized problem (discretized with the finite element method - the paper provides neither numerical applications, nor details of the implementation) for which the existence of minimizers is guaranteed, while we consider the continuous problem. Also, the author assumes that the finite element approximations satisfy some convergence hypotheses. Moreover, in our case, less regularity is required for the formulation of the inequality constraint (see in particular the remark in the proof of Theorem 2).
The decoupled problem is thus defined by means of the following functional:

$$\bar{I}(\varphi, V) = \frac{\nu}{2}\int_{\Omega} \left(T(\varphi(x)) - R(x)\right)^2 \, dx + \int_{\Omega} \mathbb{W}(V)\, dx, \tag{6}$$

with

$$\begin{cases} \mathbb{W}(V) = W(V) \ \text{ if } ||V||^2 \geq \alpha = 2\dfrac{\lambda+\mu}{\lambda+2\mu} \quad \text{and} \\ \mathbb{W}(V) = \Psi(\det V) \ \text{ si } ||V||^2 < \alpha = 2\dfrac{\lambda+\mu}{\lambda+2\mu}. \end{cases}$$

Let us now denote by $\widehat{\mathcal{W}}$ the functional space defined by $\widehat{\mathcal{W}} = \mathrm{Id} + W_0^{1,2}(\Omega, \mathbb{R}^2)$ and by $\widehat{\chi}$, $\widehat{\chi} = \left\{V \in L^4(\Omega, M_2),\ \det V \in L^2(\Omega)\right\}$. The decoupled problem consists in minimizing (6) on $\widehat{\mathcal{W}} \times \widehat{\chi}$ under the constraint $||\nabla\varphi - V||^2_{L^2(\Omega,M_2)} \leq \varepsilon$, with $\varepsilon > 0$ and $\varepsilon \in]0, \varepsilon_0]$, $\varepsilon_0 > 0$ fixed. The idea is of course to let ε go to 0. Then the following theorem holds.

Theorem 2. *Let (ε_j) be a sequence such that $\lim\limits_{j\to+\infty} \varepsilon_j = 0$. Let also $(\varphi_k(\varepsilon_j), V_k(\varepsilon_j))$ be a minimizing sequence of the decoupled problem under inequality constraint defined with $\varepsilon = \varepsilon_j$. Then there exist a subsequence denoted by $\left(\varphi_{N(\varepsilon_{\Psi\circ g(j)})}(\varepsilon_{\Psi\circ g(j)}), V_{N(\varepsilon_{\Psi\circ g(j)})}(\varepsilon_{\Psi\circ g(j)})\right)$ of $(\varphi_k(\varepsilon_j), V_k(\varepsilon_j))$ and a minimizer $\bar{\varphi}$ of $\bar{I}(\varphi)$ ($\bar{\varphi} \in Id + W_0^{1,4}(\Omega, \mathbb{R}^2)$) such that:*

$$\lim_{j\to+\infty} \bar{I}\left(\varphi_{N(\varepsilon_{\Psi\circ g(j)})}(\varepsilon_{\Psi\circ g(j)}), V_{N(\varepsilon_{\Psi\circ g(j)})}(\varepsilon_{\Psi\circ g(j)})\right) = \bar{I}(\bar{\varphi}).$$

Proof. The proof is rather long so we only give the broad lines for the sake of conciseness. Let $\varepsilon > 0$ be given, $\varepsilon \in]0, \varepsilon_0]$, $\varepsilon_0 > 0$ fixed. There exists $\widehat{\varphi_\varepsilon} \in \mathcal{W} = \mathrm{Id} + W_0^{1,4}(\Omega, \mathbb{R}^2)$ such that:

$$\inf_{(\varphi,V)\in\widehat{\mathcal{W}}\times\widehat{\chi}} \bar{I}(\varphi, V) \leq \bar{I}(\widehat{\varphi_\varepsilon}, \nabla\widehat{\varphi_\varepsilon}) = \bar{I}(\widehat{\varphi_\varepsilon}) < \inf_{\varphi\in\mathcal{W}} \bar{I}(\varphi) + \varepsilon \leq \inf_{\varphi\in\mathcal{W}} \bar{I}(\varphi) + \varepsilon_0.$$

since $W^{1,4}(\Omega, \mathbb{R}^2) \subset W^{1,2}(\Omega, \mathbb{R}^2)$. Consequently,

$$\inf_{(\varphi,V)\in\widehat{\mathcal{W}}\times\widehat{\chi}} \bar{I}(\varphi, V) \leq \inf_{\varphi\in\mathcal{W}} \bar{I}(\varphi) + \varepsilon.$$

The second part of the proof consists in taking a sequence (ε_j) such that $\lim_{j\to+\infty} \varepsilon_j = 0$. We then consider a minimizing sequence denoted by $(\varphi_k(\varepsilon_j), V_k(\varepsilon_j))$ for the decoupled problem with $\varepsilon = \varepsilon_j$. We prove that there exists $N(\varepsilon_j) \in \mathbb{N}$ such that

$$\bar{I}\left(\varphi_{N(\varepsilon_j)}(\varepsilon_j), V_{N(\varepsilon_j)}(\varepsilon_j)\right) \leq \inf_{\varphi\in\mathcal{W}} \bar{I}(\varphi) + 2\varepsilon_j \leq \inf_{\varphi\in\mathcal{W}} \bar{I}(\varphi) + 2\varepsilon_0 < +\infty.$$

Using compactness arguments (among which Rellich-Kondrachov compact embedding theorem) and Theorem 1.14 from [7] (that states that if $u_\nu \rightharpoonup u$ in $W^{1,2}(\Omega, \mathbb{R}^2)$ then $\det \nabla u_\nu \rightharpoonup \det \nabla u$ in the sense of distributions), we demonstrate the existence of a subsequence $\left(\varphi_{N(\varepsilon_{\Psi\circ g(j)})}(\varepsilon_{\Psi\circ g(j)}), V_{N(\varepsilon_{\Psi\circ g(j)})}(\varepsilon_{\Psi\circ g(j)})\right)$ such that:

$$\inf_{\varphi\in\mathcal{W}} \bar{I}(\varphi) \leq \bar{I}(\bar{\varphi}) = \bar{I}(\bar{\varphi}, \nabla\bar{\varphi}) \leq \liminf_{j\to+\infty} \bar{I}\left(\varphi_{N(\varepsilon_{\Psi\circ g(j)})}(\varepsilon_{\Psi\circ g(j)}), V_{N(\varepsilon_{\Psi\circ g(j)})}(\varepsilon_{\Psi\circ g(j)})\right).$$

We remark that we gain some regularity: indeed, $\varphi_{N(\varepsilon_{\Psi\circ g(j)})}(\varepsilon_{\Psi\circ g(j)})$ is only $W^{1,2}(\Omega, \mathbb{R}^2)$ owing to the definition of the inequality constraint but when passing to the limit when $j \to +\infty$, we prove that $\varphi_{N(\varepsilon_{\Psi\circ g(j)})}(\varepsilon_{\Psi\circ g(j)}) \rightharpoonup \bar{\varphi}$ in $W^{1,2}(\Omega, \mathbb{R}^2)$ with $\bar{\varphi} \in W^{1,4}(\Omega, \mathbb{R}^2)$.

Inspired by this theoretical result, we now turn to the discretization of the considered problem.

3.2 Numerical Scheme

The algorithm requires the evaluation of the Template T at $\varphi(x)$. We thus assume that T is a smooth mapping that has been obtained by interpolating the image data provided on the grid. As an additional convention, T is supposed to vanish outside the domain, *i.e.*, $T(x) = 0$ if $x \notin \Omega$. As suggested by Modersitzki in [17], Chapter 3, subsection 3.6.1, for the interpolation stage we apply a multiscale interpolation technique which includes a weighting parameter controlling smoothness versus data proximity. Also, for the sake of optimization, a multilevel representation of the data is adopted (see Chapter 3, section 3.7 of [17]).
We now focus on the discretization of the problem. In this purpose, we denote by H_ϵ the regularized one-dimensional Heaviside function defined by $H_\epsilon : z \mapsto$

$\frac{1}{2}\left(1+\frac{2}{\pi}\text{Arctan}\frac{z}{\epsilon}\right)$.
As seen in subsection 3.1, we overcome the difficulty of minimizing the original relaxed functional (5) by introducing an auxiliary variable V mimicking $\nabla\varphi$. The nonlinear-elasticity-based regularizer is thus applied to V and no longer to $\nabla\varphi$. We thus propose to minimize:

$$\inf_{\varphi,V} \bar{\mathcal{J}}_\epsilon(\varphi,V) + \frac{\alpha'}{2}\int_\Omega ||V-\nabla\varphi||^2\,dx \ \text{, with} \tag{7}$$

$$\begin{aligned}\bar{\mathcal{J}}_\epsilon(\varphi,V) =& \frac{\nu}{2}\int_\Omega \left(T(\varphi)-R\right)^2\,dx + \int_\Omega W(V)\,H_\epsilon\left(||V||^2 - 2\frac{\lambda+\mu}{\lambda+2\mu}\right)\,dx \\ &+ \int_\Omega \Psi(\det V)\,H_\epsilon\left(2\frac{\lambda+\mu}{\lambda+2\mu} - ||V||^2\right)\,dx,\end{aligned} \tag{8}$$

where α' is a positive constant, big enough to ensure that V and $\nabla\varphi$ are sufficiently close in the sense of the L^2-norm.

The system of optimality conditions is obtained. Numerically, the Euler-Lagrange equations in φ and V are solved using a gradient descent method, parameterizing the descent direction by an artificial time $t \geq 0$. Systems of 2 and 4 equations are obtained (solved by implicit and semi-implicit finite difference schemes - in particular, the unconditional stability of the numerical scheme in φ for fixed V is ensured), equipped with the boundary conditions $\varphi = \text{Id}$ on $\partial\Omega$.

3.3 Numerical Simulations and Discussion

We conclude the paper by presenting some medical illustrations on real data. The method is proposed for mapping a 2D slice of mouse brain gene expression data (template T) to its corresponding 2D slice of the mouse brain atlas in order to facilitate the integration of anatomic, genetic and physiologic observations from multiple subjects in a common space. Since genetic mutations and knock-out strains of mice provide critical models for a variety of human diseases, such linkage between genetic information and anatomical structure is important. The data are provided by the Center for Computational Biology, UCLA. The mouse atlas acquired from the LONI database was pre-segmented. The gene expression data were segmented manually to facilitate data processing in other applications. Some studies have developed algorithms for automatically segmenting the brain area of gene expression data. The non-brain regions have been removed to produce better matching.
The deformation must remain physically and mechanically meaningful, and reflect material properties: self-penetration of the matter (indicating that the transformation is not injective) should be prohibited. In the studied functional, there is no term preventing the Jacobian determinant from tending to 0^+. An alternative to the straight penalization of the Jacobian determinant is proposed in [5]. Their fluid model is complemented by a regridding technique ensuring positivity of the Jacobian determinant. We also refer the reader to [13]: the given

topology-preserving model is motivated by a mathematical characterization of topology preservation for a deformation field mapping two subsets of $\mathbb{Z}^2$. Note that in the present work, we did not need to resort to such methods.

The model has been tested on 4 pairs, all of size 200×200 pixels (Figs. 1, 2) (except the second one of size 220×200). For the first two tests, the data are artificially obtained from the real data used later, which enables us to compare the results of the proposed method with some of those presented in [14]. The application related to Pair 1 (Fig. 1, first row) is similar to the one performed in [14]. As suggested in [14], classical non-parametric methods such as elastic registration, linear diffusion registration, biharmonic-regularizer-based registration (see [17] for further details) fail to correctly correlate the two images, some artifacts being visible on the deformed Template (under the left ear for the observer, where the deformations are the largest). Our method qualitatively performs as the one in [14] and produces a smooth deformation field, but unlike the one in [14], is theoretically well-motivated. Also, the algorithm has been optimized; first, by capitalizing on LAPACK and Basic Linear Algebra Subprogram (BLAS) routines. Second, by parallelizing the code (we focused on the OpenMP Application Program Interface). For all the applications, the ranges of the parameters are the same (see sub-captions of Figs. 1, 2). Parameter ν balancing the fidelity term is between 1.4 and 2, the Lamé coefficient λ is set to 10 (it has no physical meaning but is related to Poisson's ratio, measure of Poisson's effect which can be regarded as the ability of a material compressed in one direction to expand in the other (two) direction(s) - this choice of λ is not physically inconsistent), while the coefficient μ is between 3000 and 5000. Parameter α' is always set to 60000. This choice gives satisfactory results. For the two remaining pairs (Figs. 2), although the Template and the Reference are of different modalities, we still use the standard L^2 distance as measure for simplicity of calculation. The algorithm produces a smooth deformation between the gene and the atlas data with a regular distribution of the Jacobian determinants, without requiring regridding steps. Also, contrary to [12] in which the deformation is mainly present near the boundaries of the brain region, here the deformation is present both near the boundary and inside the brain region. If we keep comparing our results with the ones obtained by Le Guyader and Vese in [12], for Pair 2, 4 regridding steps were necessary and the range of the Jacobian determinants was $[0.005, 28.94]$ (in [12]). For Pair 4, 3 regridding steps were necessary and the range of the Jacobian determinants was $[0.008, 10.2]$. The range of the Jacobian determinants is also larger in [14] for the same applications. In our proposed method, the Jacobian determinant thus remains closer to 1. Nevertheless, this constraint can be weakened by downplaying the role of parameter μ. The proposed model thus easily handles large deformations without requiring prohibitive computational times. In our future studies, we will examine the registration accuracy of the model when ground truth is known and will adapt it to the 3D case.

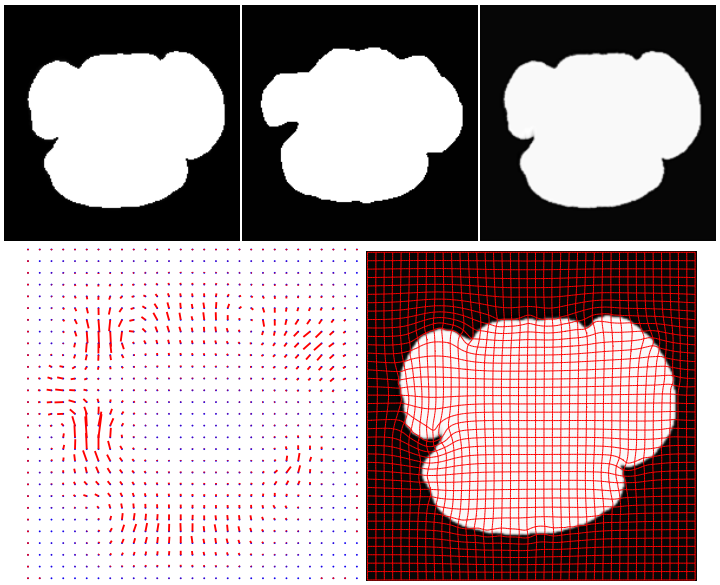

(a) Pair 1: $\nu = 2$, $\lambda = 10$, $\mu = 3000$, $\alpha' = 60000$, $\min\det\nabla\varphi = 0.09$, $\max\det\nabla\varphi = 2.47$, execution time: 1.8 s. From left to right, top to bottom: Reference R; Template T (mouse atlas and gene expression data); deformed Template; distortion map drawing the vectors from the grid points from the Reference image to non grid points after registration every 7 rows and columns; deformed grid.

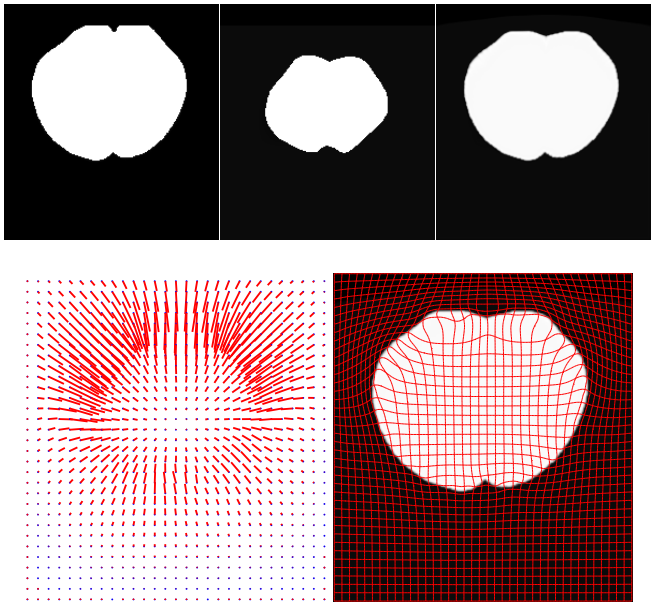

(b) Pair 2: $\nu = 1.8$, $\lambda = 10$, $\mu = 4000$, $\alpha' = 60000$, $\min\det\nabla\varphi = 0.02$, $\max\det\nabla\varphi = 2.21$, execution time: 8.4 s. From left to right, top to bottom: Reference R; Template T (mouse atlas and gene expression data); deformed Template; distortion map drawing the vectors from the grid points from the Reference image to non grid points after registration every 7 rows and columns; deformed grid.

Fig. 1: From top to bottom: Pair 1 till Pair 2.

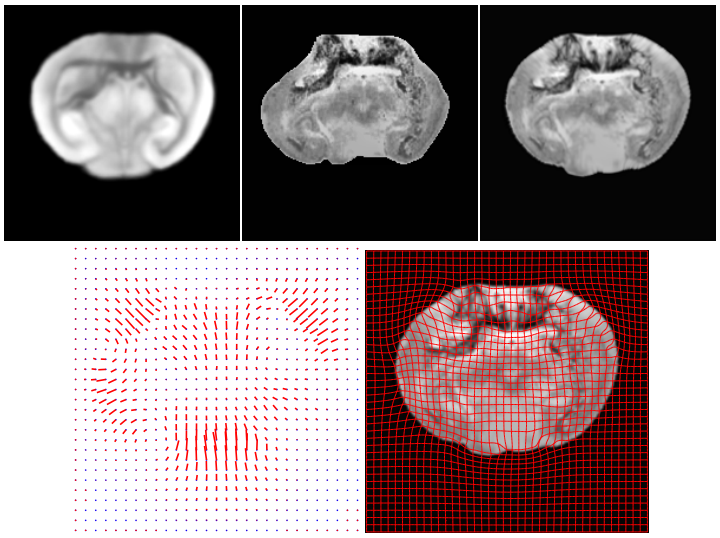

(a) Pair 3: $\nu = 2$, $\lambda = 10$, $\mu = 3000$, $\alpha' = 60000$, $\min \det \nabla\varphi = 0.008$, $\max \det \nabla\varphi = 1.96$, execution time: 1.9 s. From left to right, top to bottom: Reference R; Template T (mouse atlas and gene expression data); deformed Template; distortion map drawing the vectors from the grid points from the Reference image to non grid points after registration every 7 rows and columns; deformed grid.

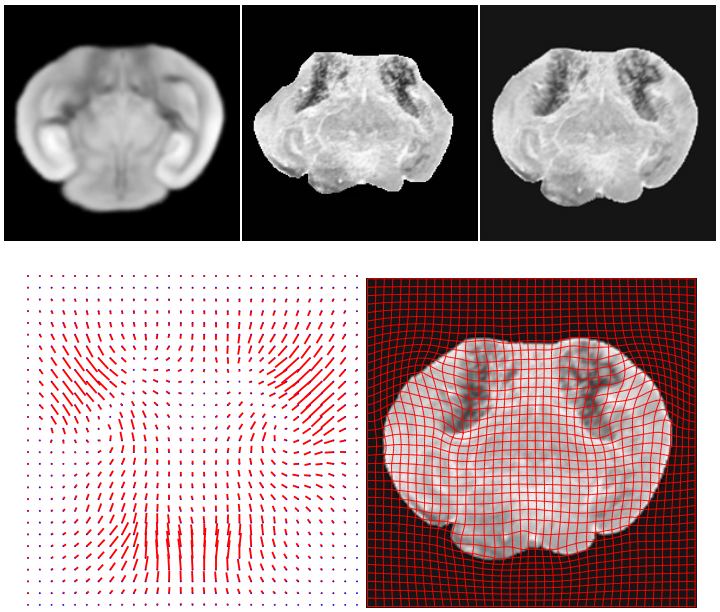

(b) Pair 4: $\nu = 1.4$, $\lambda = 10$, $\mu = 5000$, $\alpha' = 60000$, $\min \det \nabla\varphi = 0.02$, $\max \det \nabla\varphi = 1.56$, execution time: 9.5 s. From left to right, top to bottom: Reference R; Template T (mouse atlas and gene expression data); deformed Template; distortion map drawing the vectors from the grid points from the Reference image to non grid points after registration every 7 rows and columns; deformed grid.

Fig. 2: From top to bottom: Pair 3 till Pair 4.

References

1. Acerbi, E., Fusco, N.: Semicontinuity Problems in the Calculus of Variations. Arch. Rational Mech. Anal. 86, 125–145 (1984)
2. Beg, F., Miller, M., Trouvé, A., Younes, L.: Computing Large Deformation Metric Mappings Via Geodesic Flows of Diffeomorphisms. IJCV 61(2), 139–157 (2005)
3. Bousselsal, M.: Étude de Quelques Problèmes de Calcul des Variations Liés à la Mécanique. PhD thesis, Applied Mathematics, University of Metz, France (1993)
4. Broit, C.: Registration of Deformed Images. PhD thesis, Computer and Information Science, University of Pennsylvania, 1981.
5. Christensen, G.E., Rabbitt, R.D., Miller, M.I.: Deformable Templates Using Large Deformation Kinematics. IEEE Trans. Image Process. 5(10), 1435–1447 (1996)
6. Ciarlet, P.G.: Elasticité Tridimensionnelle. Masson (1985)
7. Dacorogna, B.: Direct Methods in the Calculus of Variations, Second Edition. Springer (2008)
8. Droske, M., Rumpf, M.: A Variational Approach to Non-Rigid Morphological Registration. SIAM J. Appl. Math. 64(2), 668–687 (2004)
9. Fischer, B., Modersitzki, J.: Fast Diffusion Registration. AMS Contemporary Mathematics, Inverse Problems, Image Analysis, and Medical Imaging 313, 11–129 (2002)
10. Fischer, B., Modersitzki, J.: Curvature based image registration. JMIV 18(1), 81–85 (2003)
11. Haber, E., Modersitzki, J.: Intensity Gradient Based Registration and Fusion for Multi-Modal Images. In Barillot, C., Haynor, D.R., Hellier, P. (eds.) MICCAI 2006. LNCS, vol. 3216, pp. 591–598. Springer, Heidelberg (2006)
12. Le Guyader, C., Vese, L.A.: A Combined Segmentation and Registration Framework with a Nonlinear Elasticity Smoother. Comput. Vis. Image Underst. 115(12), 1689–1709 (2011)
13. Le Guyader, C., Apprato, D., Gout, C.: On the Construction of Topology-Preserving Deformation Fields. IEEE T. Image Process. 21(4), 1587–1599 (2012)
14. Lin, T., Le Guyader, C., Dinov, I., Thompson, P., Toga, A., Vese, L.A.: Gene Expression Data to Mouse Atlas Registration Using a Nonlinear Elasticity Smoother and Landmark Points Constraints. J. Sci. Comput. 50, 586–609 (2012)
15. Marcellini, P.: Approximation of Quasiconvex Functions and Lower Semicontinuity of Multiple Integrals. Manuscripta Math. 51, 1–28 (1985)
16. Miller, M., Trouvé, A., Younes, L.: On the Metrics and Euler-Lagrange Equations of Computational Anatomy. Annu. Rev. B. Eng. 4, 375–405 (2002)
17. Modersitzki, J.: FAIR: Flexible Algorithms for Image Registration. SIAM, Philadelphia (2009)
18. Negrón Marrero, P. V.: A numerical method for detecting singular minimizers of multidimensional problems in nonlinear elasticity. Numerische Mathematik 58, 135–144 (1990)
19. Nocedal, J., Wright, S. J.: Numerical Optimization. Springer, New York (1999)
20. Rabbitt, R.D., Weiss, J.A., Christensen, G.E., Miller, M.I.: Mapping of Hyperelastic Deformable Templates Using the Finite Element Method. In: Proceedings SPIE, vol. 2573, pp. 252–265 (1995)